Int J Fract (2011) 171:169–175
DOI 10.1007/s10704-011-9596-8

ORIGINAL PAPER

Numerical simulations demonstrate that the double tapering of the spatualae of lizards and insects maximize both detachment resistance and stability

Antonio Pantano · Nicola M. Pugno · Stanislav N. Gorb

Received: 2 March 2010 / Accepted: 3 March 2011 / Published online: 13 April 2011

Abstract Many biological attachment devices of insects, spiders and geckos consist of arrays of hairs (setae), which are terminated by contact elements of different shapes. However, the most frequently observed shape is a thin plate-like spatula. In spite of a rather wide range of sizes, most spatulae of different animals are not uniform, but rather possess a gradient in thickness and width. Here we show that the spatulae of insects and geckos become gradually thinner and wider approaching the end. This geometrical effect is explained in the present paper, by using a numerical approach for the modelling of the van der Waals adhesion and friction between the contact elements and the substrate. The approach suggests that the observed negative thickness gradient contributes to the improvement of the adhesion resistance, whereas the positive width gradient increases the stability of the detachment, probably a key factor in controlling the animal walking.

Keywords Adhesion · Peeling · Gecko

A. Pantano
Department of Mechanics, Università degli Studi di Palermo, Palermo, Italy
e-mail: apantano@dima.unipa.it

N. M. Pugno (✉)
Department of Structural Engineering and Geotechnics, Laboratory of Bio-inspired Nanomechanics "Giuseppe Maria Pugno", Politecnico di Torino, Torino, Italy
e-mail: nicola.pugno@polito.it

S. N. Gorb
Department of Functional Morphology and Biomechanics, Zoological Institute at the University of Kiel, Kiel, Germany
e-mail: sgorb@zoologie.uni-kiel.de

1 Introduction

Animal's climbing ability on smooth surfaces has attracted human attention for more than two millennia (Aristotle 343 B.C.). Until the half of twenty, century, scientific observations have not permitted to well understand the capacity of geckos and insects to stay stuck motionless or running on vertical or inverted surfaces (Simmermacher 1984; Schmidt 1904; Dellit 1934, Ruibal and Ernst 1965). Only after the invention of electron microscopy, researchers have visualised the hierarchical, ranging from the nano- to the macro-scale, morphology of the animal feet (Russell 1975, 1986; Schleich and Kästle 1986; Gennaro 1969; Hiller 1968).

A typical Tokay gecko toe consists of hierarchical structures starting with macroscopic lamellae (flexible ridges, $\sim$ 1 mm long) covered by branching setae (30–130 μm long and 5–10 μm in diameter). Each seta is terminated with 100–1,000 substructures called spatulae (0.1–0.2 μm wide and 15–20 nm thick), responsible for the adhesion with the substrate. More recently, numerous studies (Autumn and Peattie 2002; Autumn 2007; Autumn and Gravish 2008; Arzt et al. 2003; Bergmann and Irschick 2005; Huber et al. 2005a,b; Autumn et al. 2000, 2006, 2007; Huber et al. 2005b)

discuss factors allowing the gecko to adhere and detach from surfaces. In particular both van der Waals attraction (Autumn et al. 2000) and capillary effects (Huber et al. 2005b) have been recognized as the key physical forces contributing to the gecko adhesion.

Also many other animals, such as beetles, flies and spiders possess similar ability to move on vertical surfaces and ceilings, and their systems are surprisingly based on a similar hierarchical organisation and spatula-like geometry (Stork 1980; Gorb 2001).

It is noteworthy that in animal groups with heavier representatives, the size of the terminal attachment elements decreases and their density increases. Studies on such biological systems have generated new ideas on the biomimetic materials science in the framework of smart adhesives (Yurdumakan et al. 2005; Haeshin et al. 2007; Pugno 2007; Pugno 2008).

Since the above mentioned animals possess tape-like terminal contact spatulae, the use of the classical Kendall approach Kendall (1975) for describing the single peeling could be appropriate. However, since the peeling approach is correct only for the uniform tape, animal spatulae, having thickness and width gradients, have more complex contact architectures and must be numerically investigated to better understand the functional principles of such biological attachment devices.

Accordingly, in the present paper, we have characterize the exact geometry of the spatulae in beetles, flies and geckos by the use of cryo scanning electron microscopy and transmission electron microscopy. Then, the observed geometries have been inserted in a numerical code for modelling the van der Waals adhesion and friction forces at the interface and thus to derive the strength and stability of the attachment. The approach suggests that the observed structural gradients may enhance resistance and stability to peeling.

2 Cryo scanning (Cryo-SEM) and transmission (TEM) electron microscopy

2.1 Cryo-SEM approach

For visualisation of the spatulae in contact with the substrate, we have used Hitachi S-4800 Scanning Electron Microscope equipped with a Gatan ALTO-2500 cryo preparation system (Cryo-SEM). We cut off feet of a non-moulting gecko (*Gekko Tokay gecko*), beetle *Gastrophysa viridula* and fly *Episyrphus balteatus*, just after dying and brought them in the contact with a clean glass surface by the use of fine forceps under a binocular microscope. The glass slides with attached feet were frozen in liquid nitrogen, transferred to the cryostage of the preparation chamber (−140 °C) and then sublimated at a temperature of −90 °C for 3 min in order to remove contamination by condensed ice crystals. The sample was coated in the frozen condition with gold-palladium (3 nm thickness) and observed at −120 °C and at a SEM accelerating voltage of 1–3 kV.

2.2 TEM approach

For the Tunneling Electron Microscope (TEM) analysis, desired pieces of animal feet were fixed for 12 h at 4 °C in 2.5% glutaraldehyde (in 0.01 M phosphate buffer at pH 7.3) and postfixed for 1 h in 1% osmium tetroxide in phosphate buffer at 2 °C. After washing, the preparations were stained for 1 h at 4 °C in 0.1% aqueous uranyl acetate solution, washed, dehydrated and embedded in a low-viscosity resin (Spurr 1969). Ultrathin sections were picked up on copper grids coated with a formvar film. Sections were stained with uranyl acetate and lead citrate and observations were made with a Philips CM10 TEM.

2.3 Spatula geometry in different animals

In the spatulae of all the three studied animals we have clearly observed similar geometrical gradients (Fig. 1). Spatulae are much thinner at their tips than at the bases. In the beetle *G. viridula* the thickness ranges from 1.4 μm to 100 nm (Fig. 1a) whereas in the fly *E. balteatus*— from 300 to 80 nm (Fig. 1b). In the Tokay gecko, spatulae are much thinner and range in their thickness from 100 to 5 nm (Fig. 1c,d). All studied spatulae are wider at their tips (Fig. 1a,c) than at the bases.

3 Numerical model

Peeling modelling of the observed single spatulae can be constructed by an *ad hoc* numerical simulation of the van der Waals forces arising at the interface and inducing both adhesion and friction.

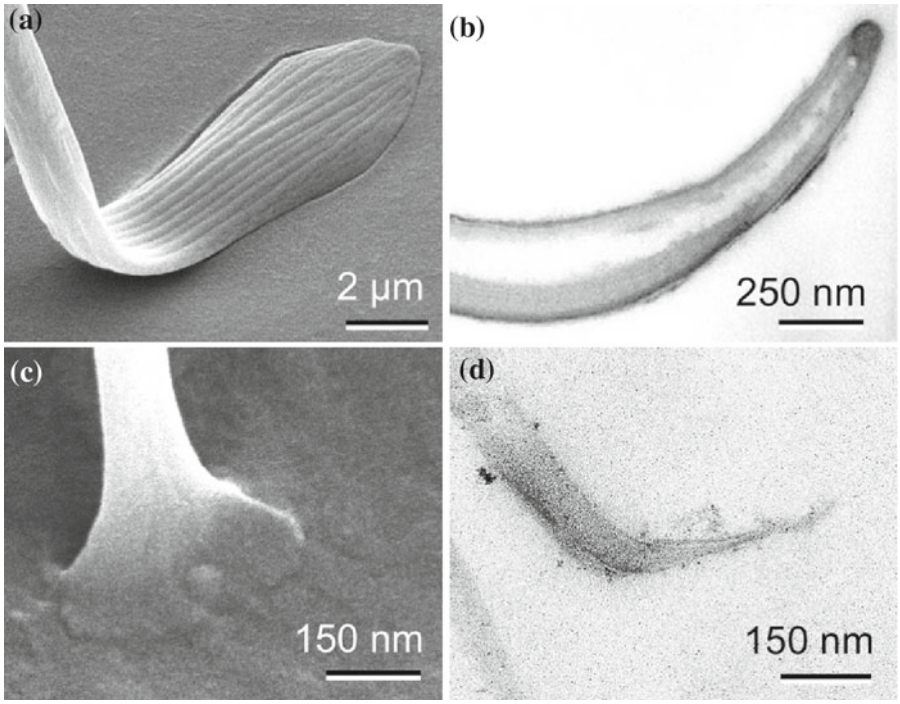

Fig. 1 Scanning (**a**, **c**) and transmission (**b**, **d**) electron micrographs of the spatulae of hairy attachment devices in insects (**a**, **b**) and lizards (**c**, **d**). **a** Beetle *Gastrophysa viridula* (Coleoptera, Chrysomelidae). **b** Fly *Episyrphus balteatus* (Diptera, Syrphidae). **c**, **d** Tokay gecko *Gekko gecko* (Reptilia, Gekkonidae). **a**, **c** Spatulae in contact with the smooth substrate. **b**, **d** Longitudinal sections of the spatulae

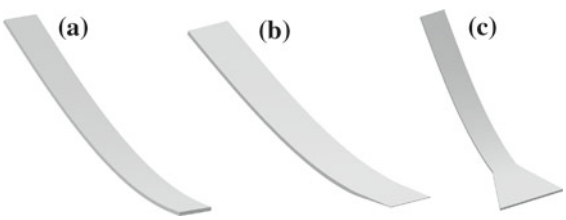

Fig. 2 Finite elements models of spatulae of different geometries. **a** Straight, **b** tapered in thickness, **c** tapered in width

3.1 Model of the spatula

The single spatula is modelled as an isotropic linear elastic continuum. The Young's modulus is assumed to be 1 GPa, which is a reasonable value for insect cuticles and gecko keratin. Three different geometries have been considered for the terminal part of the spatula: (1) straight rectangular (not tapered), (2) tapered in thickness, (3) tapered in width. The total length of the of the spatula is 1,300 nm. The total contact area was kept equal for the first two cases, but it is almost double for the model tapered in width. For the first two models, the segment of the spatula in contact with the substrate was 300 nm long and its width was 150 nm (Fig. 2a, b). For the third one, tapering in the spatula width has been applied from 150 nm at the base to 400 nm at the tip. The thickness was constant, 15 nm, for the first, and the third models (Fig. 2a, c). The second model had a thickness gradient from 15 to 2.5 nm (Fig. 2).

In Table 1 the geometry of the models are reported for the three end types.

3.2 Construction of special interaction elements

The development of an interaction element able to simulate van der Waals forces was necessary in order to study the adhesion and friction between the spatula and the substrate. Two major functional forms have been used in empirical models of the van der Waals interaction potential: the inverse power model and the Morse function model. A very widely used inverse power model is the Lennard–Jones (LJ) potential:

$$\phi_i = \frac{A}{\sigma^6}\left[\frac{1}{2}y_0^6\frac{1}{\left(\frac{r_i}{\sigma}\right)^{12}} - \frac{1}{\left(\frac{r_i}{\sigma}\right)^6}\right] \quad (1)$$

For example for the carbon–carbon system, the atom/atom non-bonded LJ potential energy has been treated by Girifalco et al. (2000) and Girifalco and Lad (1956), where $\sigma = 0.142$ nm is the C–C bond length, y_0 is a dimensionless constant, and r_i is the distance between the ith atom pair. For graphite, Girifalco and Lad (1956)

Table 1 Geometry of the models for the three end types

Geometry	Length (nm)	Width (nm)	Thickness (nm)
Straight	300	150	15
Tapered in thickness	300	150	15 initial–2.5 final
Tapered in width	300	150 initial–400 final	15

determined $A = 24.3\times10^{-79}$J m^6 and $y_0 = 2.7$. In the literature, e.g. Zhao and Spain (1989), Ruoff and Ruoff (1991), Qian et al. (2001), Hanfland et al. (1989), Boettger (1997), the LJ and local density approximation (LDA) potentials are compared by computing the equation of state (EOS) for a graphite system by assuming no relaxation within the graphene plane. Two graphene sheets (in AA and AB registry, respectively) are considered. The in-plane geometry is held fixed, and the inter-layer distance is changed. The computed pressure is plotted as a function of the volume change. The results are compared with published experimental data Zhao and Spain (1989); Hanfland et al. (1989) and with the *ab initio* treatment Boettger (1997). The models provided good fits to the experimental data, but the LDA model shows too strong attractive interaction at distances greater than 0.34 nm.

The resulting expression for the pressure as a function of the inter-layer distance computed from the LJ

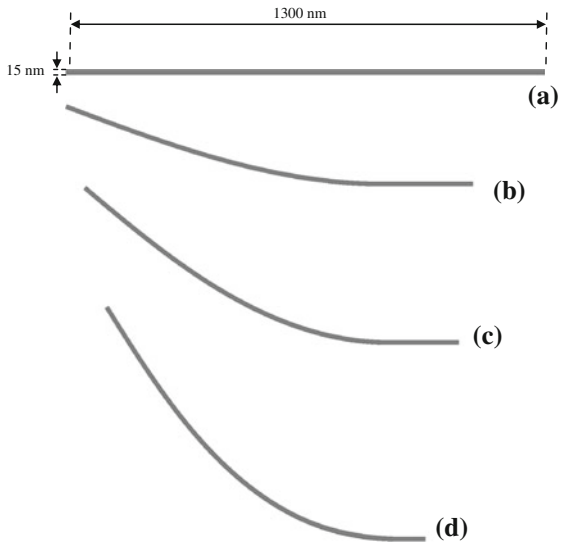

Fig. 3 Simulation of the peeling of the single spatula. **a** An initial undeformed configuration; progression of the peeling at different heights of the end of the spatula: 240 nm (**b**), 481 nm (**c**), 723 nm (**d**)

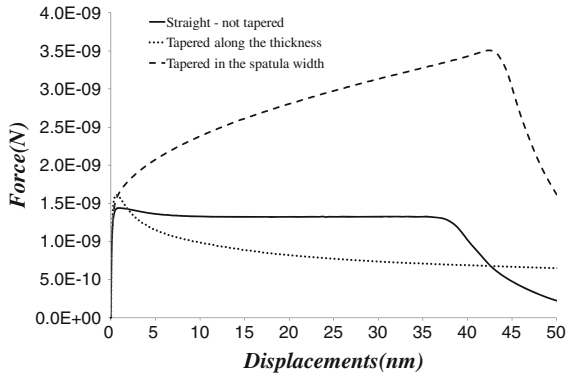

Fig. 4 Force versus displacement curves of the free-ends of the spatula tips for the investigated three different geometries. Note that the increment of the adhesion force for the thickness tapered geometry is theoretically expected (Pugno 2008), as well as we expected the positive and nearly constant variation of the force with respect to the displacement δ, since $\mathrm{d}F(z)/\mathrm{d}z \sim \mathrm{d}b(z)/\mathrm{d}z > 0$ and roughly $\delta \sim z$

potential has been implemented in an ABAQUS software (V 6.8, Dassault Systèmes, Providence, RI, USA) user subroutine for simulating the van der Waals forces. The pressure/inter-layer-distance relation calculated in Zhao and Spain (1989) has been adopted:

$$p(\alpha) = \frac{\Psi}{6}\left[\left(\frac{d_0}{\alpha}\right)^{10} - \left(\frac{d_0}{\alpha}\right)^{4}\right] \tag{2}$$

Here p is the pressure, α is inter-layer distance, d_0 is the equilibrium distance and Ψ is a characteristic tension. These parameters depend on the interacting materials; in the case of the gecko's spatula one of the two materials is known but the other changes according to where the gecko is walking. In the present simulations we have assumed the following values: $d_0 = 0.34$ nm and $\Psi = 10$ MPa in order to model a maximum tensile adhesive stress of about 0.54 MPa, as suggested by direct experimental observations, see Pugno (2007).

The initial boundary conditions are determined by the frictional shear strength. Friction between the spatula and the substrate has been implemented in the inter-

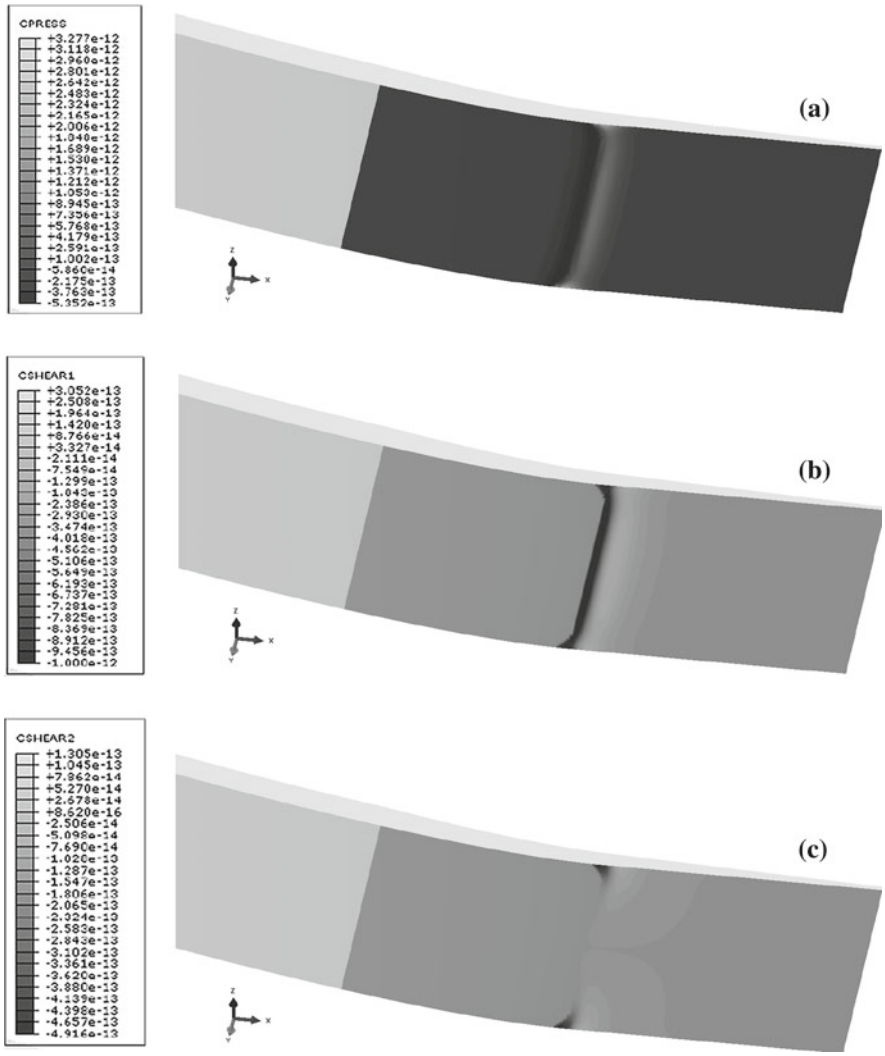

Fig. 5 Interface adhesive normal (**a**) and shear longitudinal (**b**) or transversal (**c**) stresses (in N/nm^2), as numerically computed at the incipient peeling, for the thickness tapered geometry

action element in terms of a maximum shear stress limit. This friction model, regardless of the magnitude of the contact pressure, allows the sliding if the magnitude of the equivalent shear stress reaches its maximum value. In the case of the gecko's spatula interacting with the substrate, the maximum achievable value of the shear stress is assumed to be of 1 MPa.

In the ABAQUS software, the subroutine UINTER is used to define the constitutive interaction between two deforming surfaces. The interface is taken to be massless. The developed interaction elements have been used at the interface spatula-surface.

3.3 Numerical simulations

In order to reproduce the right initial boundary conditions for the peeling test, the initially undeformed spatula lies straight on the substrate. Then the free-end of the spatula is gradually raised applying a given vertical displacement. Starting with an already bent spatula would have ignored the bending energy stored in the spatula. In the Fig. 3, the gradual deformation of the spatula is shown. The van der Waals interactions are present only in the last 300 nm of the spatula, which is 1,300 nm long for the three models. Figure 3a shows an initial undeformed configuration. Figure 3b–d shows

Table 2 Contact area, peeling force, and energy dissipated for the three end types

Geometry	Contact area (nm^2)	Force (nN)	Energy (nN nm)
Straight	$300 \times 150 = 45,000$	1.44	59.2
Tapered in thickness	$300 \times 150 = 45,000$	1.61	75.6
Tapered in width	$300(400 + 150)/2 = 82,500$	3.51	151.4

progression of the peeling; in the different Figures the imposed vertical displacement at the end of the spatula is gradually incremented reaching respectively the following heights: 240 nm (b), 481 nm (c) and 723 nm (d).

In Fig. 4, the force versus displacement curves of the spatula free-ends are reported for the three investigated geometries. It can be noticed that, for the studied configurations the force necessary to start the peeling can change because of the gradients. Both the tapering increase the peeling force (with respect to the straight-rectangular spatula tip). The tip tapered in width is stronger than the straight-rectangular spatula tip. However, more than the expected [according to classical peeling theory the detachment force F is proportional to the width b and thus for a tapered geometry we expect $F(z) \sim b(z)$] increment in the adhesion force we note that theoretically $\mathrm{d}F(z)/\mathrm{d}z \sim \mathrm{d}b(z)/\mathrm{d}z > 0$ and thus that the positive width gradient implies the stability of the detachment process, probably a key for the safe control of the animal walking. Finally, in Fig. 5, the interface adhesive shear stresses and normal stress are depicted as an example for the thickness tapered geometry.

A numerical evidence is that the spatula tapered in thickness shows a detachment force that is higher than that of the straight-not tapered geometry. This is probably a consequence of the reduced stress concentration at the interface imposed by the tapering, as suggested in Pugno (2008): the tapering in thickness enhances the peeling force of ~12%.

According to our simulations, we infer that biological attachment systems of insects and lizards have convergently developed similar contact geometries optimised for strong and stable, thus controllable, adhesion. This optimal geometry is the spatula with the thickness tapering and width gradient. In addition to the stronger resistance to peeling, extremely small thickness of the spatula end contributes to a better matching of the contact element to the substrate (Gao et al. 2005; Pugno and Lepore 2008a; Pugno and Lepore 2008b), which makes such geometry more robust to the surface roughness. Increase in the spatula width leads to the self-stabilization during the peeling process (peeling will not catastrophically propagate further to the spatula end, which will be the case for narrowing spatulae).

In Table 2 the contact area, the peeling force, and the energy dissipated are reported for the three end types.

4 Conclusions

The results of the simulations suggest that the observed tapering in the thickness and width are both useful for improving walking ability. In particular, we have numerically demonstrated that the observed negative thickness gradient contributes to the improvement of the detachment resistance, whereas the positive width gradient increases the stability of the detachment, probably a key factor in controlling the animal walking. Thus, biological attachment systems of insects and lizards could have convergently developed similar contact geometries optimised for strong and stable, thus controllable, adhesion.

Acknowledgments NMP is supported by the Piedmont Contract Metregen (2009–2012), Metrology on a cellular and macromolecular scale for regenerative medicine. SG is supported, as part of the European Science Foundation EUROCORES Programme FANAS, by funds from the German Science Foundation DFG (contract No. GO995/4-1) and the EC Sixth Framework Programme (contract No. ERAS-CT-2003-980409).

References

Aristotle (343 B.C.) Historia animalium, http://etext.virginia.edu/toc/modeng/public/AriHian.html

Arzt E, Gorb S, Spolenak R (2003) From micro to nano contacts in biological attachment devices. Proc Natl Acad Sci USA 100:10603–10606

Autumn K (2007) Gecko adhesion: structure, function, and applications. MRS Bull 32:473–478

Autumn K, Dittmore A, Santos D, Spenko M, Cutkosky M. (2006) Frictional adhesion: a new angle on gecko attachment. J Exp Biol 209:3569–3579

Autumn K, Gravish N (2008) Gecko adhesion: evolutionary nanotechnology. Phil Trans Roy Soc A 366:1575–1590. http://rsta.royalsocietypublishing.org/

Autumn K, Hsieh ST, Dudek DM, Chen J, Chitaphan C, Full JR (2007) Dynamics of geckos running vertically. J Exp Biol 209:260–272

Autumn K, Liang YA, Hsieh ST, Zesch W, Chan WP, Kenny TW, Fearing R, Full RJ (2000) Adhesive force of a single gecko foot-hair. Nature 405:681–685

Autumn K, Peattie AM (2002) Mechanisms of adhesion in geckos. Int Comp Biol 42:1081–1090

Bergmann PJ, Irschick DJ (2005) Effects of temperature on maximum clinging ability in a diurnal gecko: evidence for a passive clinging mechanism? J Exp Zool 303A:785–791

Boettger J (1997) All-electron full-potential calculation of the electronic band structure, elastic constants, and equation of state for graphite. Phys Rev B 55(17):11202–11211

Dellit WD (1934) Zur anatomie und physiologie der geckozehe. Z Naturwiss 68:613–656

Gao H, Wang X, Yao H, Gorb S, Arzt E (2005) Mechanics of hierarchical adhesion structures of geckos. Mech Mater 37:275–285

Gennaro JGJ (1969) The gecko grip. Nat Hist 78:36–43

Girifalco LA, Hodak M, Lee RS (2000) Carbon nanotubes, buckyballs, ropes, and a universal graphitic potential. Phys Rev B 62(19):13104–13110. http://prb.aps.org/

Girifalco LA, Lad RA (1956) Energy of cohesion, compressibility, and the potential energy functions of graphite system. J Chem Phys 25(4):693–697. http://jcp.aip.org/

Gorb SN (2001) Attachment devices of insect cuticle. Kluwer Academic, Dordrecht

Haeshin L, Bruce PL, Phillip BM (2007) A reversible wet/dry adhesive inspired by mussels and geckos. Nature 448: 338–341

Hanfland M, Beister H, Syassen K (1989) Graphite under pressure: equation of state and first-order Raman modes. Phys Rev B 39(17):12598–12603

Hiller U (1968) Untersuchungen zum feinbau und zur funktion der haftborsten von reptilien. Z Morphol Tiere 62:307–362

Huber G, Gorb SN, Spolenak R, Arzt E (2005a) Resolving the nanoscale adhesion of individual gecko spatulae by atomic force microscopy. Biol Lett 1:2–4

Huber G, Mantz H, Spolenak R, Mecke K, Jacobs K, Gorb SN, Arzt E (2005b) Evidence for capillarity contributions to gecko adhesion from single spatula nanomechanical measurements. Proc Natl Acad Sci USA 102:16293–16296

Kendall K (1975) Thin-film peeling-the elastic term. J Phys D Appl Phys 8:1449–1452. http://iopscience.iop.org/0022-3727

Pugno NM (2007) Towards a spiderman suit: large invisible cables and self-cleaning releasable super-adhesive materials. J Phys: Condens Matter 19:395001

Pugno NM (2008) Spiderman gloves. Nano Today 3:36–42

Pugno N, Lepore E (2008) Observation of optimal gecko's adhesion on nanorough surfaces. Biosystems 94:218–222

Pugno N, Lepore E (2008) Living tokay geckos display adhesion times following the Weibull statistics. J Adhesion 84:949–962

Qian D, Liu WK, Ruoff RS (2001) Mechanics of C60 in nanotubes. J Phys Chem B 105:10753–10758

Ruoff RS, Ruoff AL (1991) The bulk modulus of Ceo molecules and crystals: a molecular mechanical approach. Appl Phys Lett 59(13):1553–1555

Russell AP (1975) A contribution to the functional analysis of the foot of the Tokay, Gekko gecko (Reptilia: Gekkonidae). J Zool Lond 176:437–476

Russell AP (1986) The morphological basis of weight-bearing in the scansors of the tokay gecko (Repitilia: Sautia). Can J Zool 64:948–955

Ruibal R, Ernst V (1965) The structure of the digital setae of lizards. J Morphol 117:271–294. http://onlinelbrary.wiley.com/journal/10.1002/(ISSN)1097-4687

Schleich HH, Kästle W (1986) Ultrastrukturen an gecko-zehen (Reptilia: Sauria: Gekkonidae). Amphib Reptil 7:141–166

Schmidt HR (1904) Zur anatomie und physiologie der geckopfote. Z Naturwiss 39:551–563

Simmermacher G (1884) Untersuchungen über haftapparate an tarsalgliedern von insekten . Zeitschr Wiss Zool 40:481–556

Spurr AR (1969) A low-viscosity epoxy resin embedding medium for electron microscopy. J Ultrastruct Res 26:31–43

Stork NE (1980) Experimental analysis of adhesion of Chrysopolina polita (Chrysomelidae: Coleoptera) on a variety of surfaces. J Exp Biol 88:91–107

Yurdumakan B, Raravikar NR, Ajayanm PM, Dhinojwala A (2005) Synthetic gecko foot-hairs from multiwalled carbon nanotubes. Chem Commun 30:3799–3801

Zhao YX, Spain IL (1989) X-ray diffraction data for graphite to 20 GPa. Phys Rev B 40(2):993–997. http://prb.aps.org/